Kurdish Studies
May 2024
Volume: 12, No: 4, pp. 1018-1029
ISSN: 2051-4883 (Print) | ISSN 2051-4891 (Online)
www.KurdishStudies.net

DOI: 10.53555/ks.v12i4.3102

Biosynthesis And Wound Contraction Efficacy Of Zinc Oxide Nanoparticles Using Leaf Extract Of *Syzygium Cumini* (Linn.)

Hafsa Waheed[1], Bisma Rauff[2], Asma Ahmed[3]*, Rehana Badar[4], Samra Hafeez[5], Bilal Ishaq[6], Nadeem Iqbal[7]

[1,3*,4,5]Institute of Molecular Biology and Biotechnology, The University of Lahore, Lahore, Pakistan
[2]Department of Biomedical Engineering, University of Engineering and Technology (UET), Lahore, Narowal Campus, Punjab Pakistan
[4]Department of Biological Sciences, Superior University, Lahore, Punjab, Pakistan.
[6]Department of Chemistry Superior University, Lahore Pakistan
[7]Microtech Chemicals and Minerals, Kasur, Punjab, Pakistan

***Corresponding author:** asma.ahmed@imbb.uol.edu.pk

ABSTRACT
Current study was designed to evaluate the wound healing potential of leaf extracts of *Syzygium cumini* (Linn) and effectiveness of zinc oxide nanoparticles against wounds. Number of studies are already available on the plant extracts and nanoparticles against wound healing, focus of present study highlights the role of *S.cumini* for healing and presents the comparative analysis when drug was used at mg/ml and at nano range. Bio-fabricated zinc oxide nanoparticles (BZnO NPs) were synthesized via green route and were further characterized using UV-Vis spectroscopy, FTIR, XRD and SEM. Efficacy of these NPs were assessed against excision wounds using albino Wistar rats (both genders, 250-300 g) and the data was recorded in the interval of seven, fourteen and twenty-one days. For the synthesis of zinc oxide nanoparticles 10 mL of 1 mM $ZnSO_4.7H_2O$ was mixed with 3 mL of *S. cumini* leaf extract, and the reaction mixture was stirred at 80°C using magnetic stirrer for 2 hours. A clear change in color of the mixture (pale yellow to whitish) confirmed the synthesis of BZnO particles while UV-Visible analysis presented a sharp peak at 378 nm which confirmed the synthesized particles in nanoscale. The hexagonal wurtzite structure of BZnO nanoparticles through XRD analysis gave distinct peaks at 2θ position. The average size was around 70 nm with irregular shape of particles. Among all extracts, aqueous extract of *S. cumini* Linn. was found excellent reducing agent for the synthesis zinc oxide nanoparticles, while statistically analyzed results (at $p \leq 0.05$) showed that among all plant, after day 07, day 14 and day 21 also showed that *S. cumini* (Linn.) (42.5 %, 87.5 % and 100 % respectively) showed significant wound contraction in female rats as compared to male rats, while its n-Hexane extract has least significant effects. Nanoparticles have wound healing potential at all concentration, but it was maximum wound contraction after 14 days of biogenic nanoparticle application which remained continued till third week of particle application. Current study can be used as basic study for the isolation of active compound behind it so that it could be used for the formulation of curative bandage to cure excision wounds.

KEY WORDS: *Syzygium cumini* Linn., Zinc nanoparticles, Excision wounds

INTRODUCTION

Wound healing is the process by which the body repairs and replaces damaged or destroyed tissues and cells of body. Which particularly involves multiple stages, including hemostasis, inflammation, proliferation, and remodeling. Wound healing can be classified into primary and secondary healing, depending on the severity of the wound and the presence of complications. Effective wound healing requires a coordinated effort of various cellular and molecular mechanisms, and any disruptions can lead to abnormal healing or complications.

Wound healing is a complicated biological process that consists of blood coagulation, inflammation, proliferation, and remodeling. The living body switches the damaged or injured tissue by this complex and active process. Healing gets slowed down under certain pathological conditions such as heavy blood loss, microbial infection, or diabetes. Therefore, it is important to get wound treated instantly with suitable handling. So, for the wound healing process, wound dressings are one of the most important and major materials used (Mohandas *et al*., 2015). Wounds are generally classified according to the underlying cause of the development of wounds. In acute wounds, there is tissue damage/injury that generally occurs through an orderly and time-reparative phase that results in the anatomical and functional integrity being restored sustainably. Acute wounds are typically caused by the cuts or surgical incisions. In closed wounds, the blood escapes from the circulatory system but stays inside the body. It becomes evident in the form of bruises. Blood leaks from the body through an open wound and bleeding is clearly noticeable. The open wound may be divided further into categories according to the source causing the wound. Incised wound is a wound with no loss of tissue and minor damage to tissue. It is caused primarily by sharp objects like a scalpel or knife. Since dirt may penetrate deep into the wound, chances of infection are common in them. Chronic wounds are wounds that have not gone through the usual healing stages and hence reach a state of pathologic inflammation. They need extended healing time (Sharma *et al.,* 2021).

Syzygiumcumini(Linn.) has been traditionally used as a medicinal plant. Different parts of the plant (for example bark, leaves, seeds, and fruit) have been employed in the treatment of various diseases. *S.cumini*(Linn.) fruit juice has been utilized, orally, to treat gastric complaints, diabetes, and dysentery. *S.cumini*(Linn.) seeds have been applied externally to treat ulcers and sores, and powdered seeds with sugar have been given orally to combat dysentery. Powdered seeds have been reported to be effective against diabetes. *S.cumini*(Linn.) leaves were cooked in water (concentration of 2.5 g/L) and drunk daily, where 1 L has been reported to be effective against diabetes. The juice of leaves has been used as an antidote in opium poisoning, and an oral intake of leaves for 2–3 days has been reported to be effective in reducing jaundice in adults and children. Traditionally, *S.cumini*(Linn.) leaves juice along with mango leaves and myrobalan fruit administered with honey and goat milk has been used also to combat dysentery, whereas bark decoction of *S.cumini*(Linn.) with water has been used to treat diabetes, dysentery, to increase appetite, to achieve sedation, and to relieve headache when taken orally. Bark decoction has been given to females with recurrent miscarriages. *S.cumini*(Linn.) bark juice with buttermilk has been reported to treat constipation, whereas an intake in the morning has been claimed to stop blood discharge in feces (Qamar *et al.,* 2022).

Nanoscience and nanotechnology indeed represent cutting-edge fields with vast potential across various disciplines. Their ability to manipulate matter at the nanoscale level is a great platform or opportunity for innovation and advancement. By deep understanding and having abilities for the control synthesis of these substances and materials at such tiny or minute dimensions, researchers can develop novel materials, devices, and systems with unprecedented properties and functionalities. Advancement in the field of production and synthesis at such great control and tiny level is termed as nanotechnology (Santhoshkumar et al*.,* 2017). This is no doubt interdisciplinary field of science and nanotechnology which allow numerous other fields of science such as biology, physics, chemistry, and materials science, which are the leading sciences for discoveries and applications(Divya et al*.,* 2018). Nanoparticles are playing an important part in the field of medicine, drug delivery, imaging, and diagnostics which is offering more targeted and efficient treatments while minimizing side effects. Similarly, in materialsciences, nanomaterials had great mechanical, electrical, and optical properties that can revolutionize industries ranging from electronics to energy(Karthika *et al.,* 2017) (Benelli *et al*., 2018). Indeed, the application of nanoparticles in agriculture holds significant promise, particularly for subsistence and organic farmers aiming to enhance crop productivity while minimizing environmental impact. Here are some potential applications of nanoparticles in agriculture(Badar et al., 2023).

There are various method for the synthesis of these nanoparticles, such as chemical, physical, and biological methods (Vijayakumar *et al*., 2016; Ishwarya *et al*., 2018). However the synthesis of nanoparticles using microorganisms and plants is marked as the green synthesis, which surely offers several distinctive features such as environmental sustainability and cost-effectiveness (Singh *et al*., 2017; Banumathi *et al*., 2017). To produce nanoparticles method of green synthesis is sustainable and environmentally friendly, which is also in line with the principles of green chemistry and sustainable development. By harnessing the power of nature, researchers can develop innovative nanomaterials with minimal environmental impact, contributing to a cleaner and healthier planet.

The most important feature of these nanoscale particles is their larger surface-to-volume ratio which is responsible for the increase in their efficacy, and environmental sustainability. These are the most important features which made these particles more effective and common. Which means that smaller quantities of material are required to achieve greater effectiveness, making nanoscale particles a more efficient and economical choice compared to larger particles. The most prominent feature of these particles is a greater surface area relative to large size particles due to which they had greater potential to reach at the target site, which reduces the need of material at large quantity. This makes them a more efficient, cost-effective, and environmentally friendly option (Vijayakumar *et al*., 2016). No doubt these particles are becoming a material of choice due to having characteristic properties such as catalysis, water treatment, energy storage, medicine, agriculture, etc. (Khot et al. 2012; Gajanan et al., 2018 and Bratovcic, 2019). Nanomaterials possess two distinct properties that set them apart from their larger counterparts like surface effects and quantum effects. These unique properties make nanomaterials significant and confer advantages that aren't observed in the same materials at larger dimensions. Actually the small size of nanomaterials gives rise to both of the characteristic features, due to which these are commonly being in use for vast applications (Gade et al., 2010).

The conventional physical and chemical methods of synthesizing Zinc Oxide nanoparticles have several drawbacks, including high costs, toxic byproducts, and stringent conditions of pressure and temperature. To overcome these limitations, there is a growing need for sustainable and environmentally friendly approaches. Green synthesis methods have emerged as a viable alternative, offering a cost-effective and eco-friendly route to nanoparticle synthesis, free from harmful byproducts and extreme conditions. In order to over the challenges due to other methods of synthesis, green synthesis had attained significant importance, providing a sustainable and justifiable approach to nanoparticle synthesis, making it cost-effective, environmentally friendly, free from toxic byproducts (Sharma *et al.,* 2020).

S.cumini Linn. has been utilized globally as a natural remedy for various ailments since long time. Its effectiveness in treating inflammation, diabetes, diarrhea, ulcers, and cancer has been well-documented. Preclinical studies have also revealed its anti-neoplastic, radio-protective, and chemo-preventive properties. The Jamun tree is a rich source of bioactive compounds, including ellagic acid, glucoside, anthocyanins, kaempferol, and myrecetin, which are present in its leaves, fruits, barks, roots, and stems. These compounds contribute to its immense potential as a source of healthy

nutrition and medicine, with pharmacological effects that include antidiabetic, antimicrobial, antioxidant, central nervous system activity (CNS), chemo-preventive, (Singh et al., 2019).

METHODOLOGY

Study site

Present experimental analysis was performed at the animal house of Institute of Molecular Biology & Biotechnology (IMBB), The University of Lahore, Lahore, and Punjab, Pakistan. All the materials utilized for the present research work were of analytical grade.

Experimental plant

Fresh identified leaves of *S. cumini*(GC Herb. Bot. 3976)were used as an experimental material.

Preparation of plant extract

80 mesh powder of *S. cumini* (Linn.) leaves was measured by weighing balance and then dissolved in n-hexane in 1: 10 ratio in a glass bottle, followed by the shacking of mixture for 24 hours at room temperature. Then filtrate was separated by centrifugation at 15000 rpm for 15 minutes, followed by filtration through Wattman filter paper 1.0 to collect n-hexane extract of *S. cumini* (Linn.) leaves. The residue was redissolved in ether, ethanol and finally distilled water (1:10 ratio) respectively and repeated the methods of shaking and filtration to collect ether, ethanolic and water extracts (Asma *et al.*, 2015).

Synthesis of ZnO Nanoparticles

Zinc oxide nanoparticles were synthesized via a green route using an aqueous solution of zinc sulfate heptahydrate (ZnSO4.7H2O) and leaf extract of *S. cumini* (Linn.). for that 10 mL of 1 mM $ZnSO_4.7H_2O$ was mixed with 3 mL of *S. cumini* leaf extract, and the reaction mixture was stirred at 80°C using magnetic stirrer for 2 hours. While the reaction mixture was continuously monitored to note the change in color. The mixture was then centrifuged at 6000 rpm for 15 minutes, and the resulting particles were washed further four times with distilled water to remove impurities. The washed particles were subsequently dried in a hot air oven at 120°C for 1 hour to yield the final ZnO nanoparticles, which were then stored for further characterization and analysis. The characterization of the zinc oxide nanoparticles using various analytical techniques were performed as a confirmational studies.

Characterization of ZnO Nanoparticles

Characterization of prepared nanoparticles was carried out though; UV-Vis Spectrophotometry; Fourier Transform Infrared Spectroscopy (FTIR); X-ray diffraction (XRD) and Scanning Electron Microscopy (SEM) analysis

Zinc oxide nanoparticles were sonicated in distilled water for about 15 minutes and wavelength was recorded between 300-800 nm using Thermoscientific, Multiskan Sky plate reader (Mahamuni*et al.*, 2018). FTIR analysis was performed to assess the presence of active components. Results were recorded in the range of 1000 to 4000 cm^{-1} (Dobrucka*et al.*, 2016). X-ray diffraction pattern of the dried ZnO NPs were carried out using PANalyticalXpert powder diffractometer (Malvern) for the determination of shape and average size of green nanoparticles.

The average crystallite size of ZnO NPs was determined from the highest intense/narrower peak using Debye Sherrer's equation:

$$D = k\lambda / \beta\cos\theta$$

Where, D is crystallite size of nanoparticles, k is Sherrer's constant, which is 0.94, λ is the wavelength of X-ray sources used in XRD (1.5406Å), β is full width at half maximum (FWHM) of diffraction peak. θ refers to Bragg's angle. The most intense peak was chosen which is <010> and crystalline size of synthesized ZnONPs was determined around 21.63 (Bala *et al.*, 2022). For further confirmations SEM analysis of prepared nanoparticles was performed using Carl Zeiss (model: FE-SEM sigma 500 VP) to assess the surface morphology, shape, and size of ZnO NPs.

Animal selection

After ethical approval (Approval No: USM/Animal Ethics approval/2009), adult male and female albino rats (250-300gm) had been housed in standard stainless-steel cages separately to avoid mating, at controlled room temperature and 60-70 % relative humidity and fed with standard laboratory diet with free access to water. Sick and feeble rats were excluded from the study. Animals were divided in following groups.

Table 1 Different groups of animals for *in vivo* experiment

Groups		Treated with
1	Vehicle	Wounded treated with water
2	Negative Control	Wounded (untreated)
3	Positive control	Wounded treated with puyodine
4	Experimental	n-hexane extract
5		ether extract
6		ethanolic extract
7		water extract
8		Zinc oxide nanoparticle

Where Vehicle is the wounded animal treated with water, negative control was left untreated and positive control was treated with known drug (puyodine ointment), while group 4-7 was kept as an experimental treated with plants extract (*S. cumini* Linn.) and group 8 was treated with ZnO NPs.

Treatment and Excision wound formation on Rats

After induction of anesthesia (40 mg/Kg ketamine), a wound (2 × 2 cm) was made by a scalpel, which removed all cutaneous layers of animal. Then rats were randomly divided into above groups (Table 1) and applied the relevant treatments to the wound bed for 14 days. On day 7, the wound contracture (%) was measured by tracing the wound on transparent paper and a permanent marker. Recorded wound areas were measured using 1.0 mm^2 scale of graph paper. Changes in wound area were evaluated after 07, 14 and 21 days, by giving an indication of the rate of wound contraction period. The evaluated surface area was used to calculate the percentage of wound contraction by using following formula, by taking initial size of the wound as 100% **(**Sudheesh *et al.,* 2012).

$$\text{Wound contracture (\%)} = \frac{\text{(Wound area on 1st day} - \text{Wound area on last day)}}{\text{Wound area on 1st day} \times 100.}$$

Statistical analysis

Data has been analyzed through Two-way ANOVA, followed by the calculation of means and standard deviation (SD) through GraphPad 8.0 and results has been expressed as mean± SD.

RESULTS

Identified plants was *Syzygium cumini* (Linn.) (GC Herb. Bot. 3976).

Synthesis of Zinc Oxide Nanoparticles

A change in color of reaction mixture from pale yellow to whitish was the first clear indication of zinc oxide nanoparticles (BZnO NPs).

CHARACTERIZATION

UV-vis. Spectroscopic Analysis

A sharp peak was obtained at 378 nm by UV analysis of experimental particles which confirmed that the synthesized particles were in nano scale range (Figure 1 A). While the band gap energy of BZnO NPs was recorded 3.6 eV (Figure 1 B).

FTIR Analysis

Figure (2) showed the presence of active constituents which were due to the plant extracts. A clear and sharp peak at 2920.85 was due to C-H stretching, while peak positions at 3425.15 and 1433.07 were due to strong O-H stretching. Peaks at 1629.07 and 1112.53 were attributed to the presence of C=C and C-O stretching.

XRD Analysis

The pattern of synthesized ZnO NPs clearly indicated the crystalline nature of particles while the diffracted intensities were recorded from 20° to 80° at 2θ. The observed sharp diffraction peaks at 2θ values 31.7, 34.38, 36.18, 47.44, 56.54, 62.98 and 67.8 degrees. These peaks (100), (002), (101), (102), (110), (103) and (112) correspond to JCPDS Card NO. 03-065-2880 confirmed that they were in lattice planes showing hexagonal wurtzite structure (Figure 3).

SEM Analysis

Images recorded from SEM analysis confirmed that the prepared green nanoparticles were in hexagonal shape agglomerated together (Figure 4). These particles were irregular and rough in appearance with average size ranges 25-45 nm.

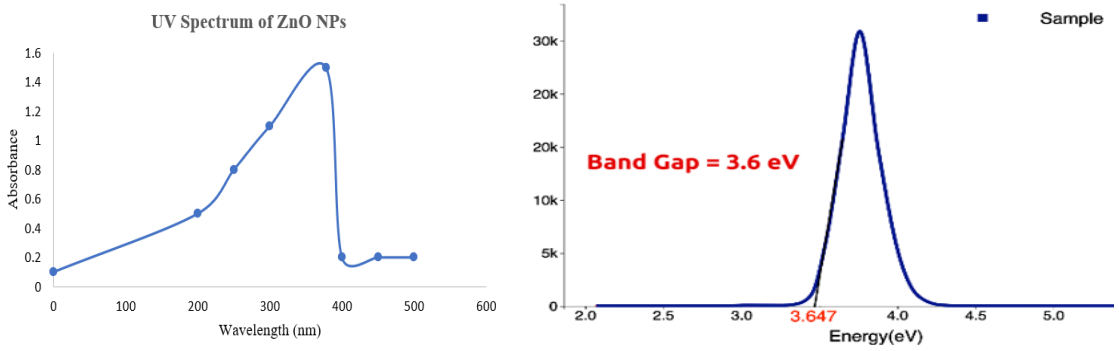

Figure 1 (A) UV Spectrum (B) Band energy gap calculated by tauc plot of bio fabricated BZnO nanoparticles.

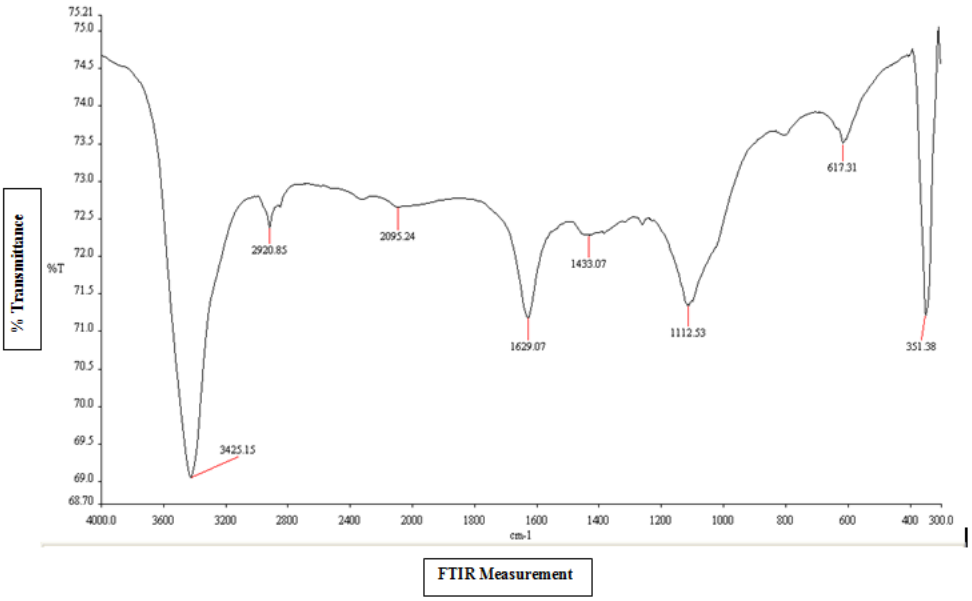

Figure 2 FTIR spectrum of bio-fabricated ZnO nanoparticles

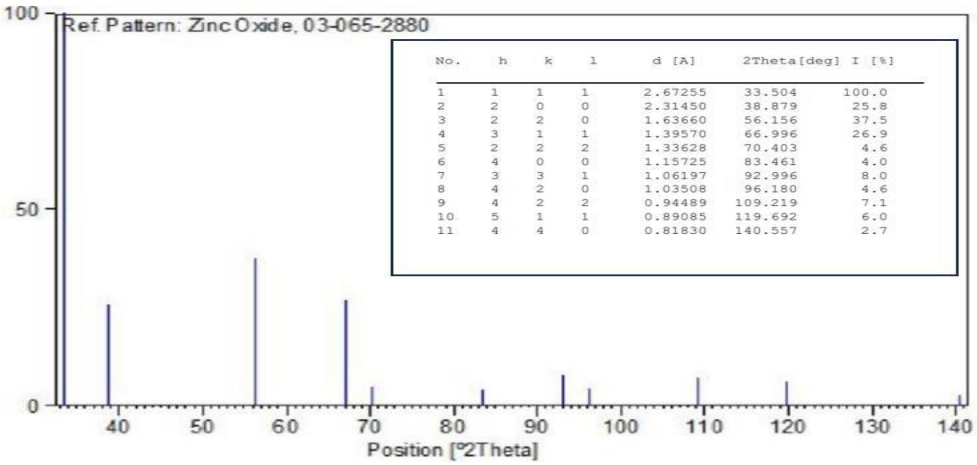

Figure 3 XRD Analysis presenting JCPDS Card NO. 03-065-2880 of BZnO NPs

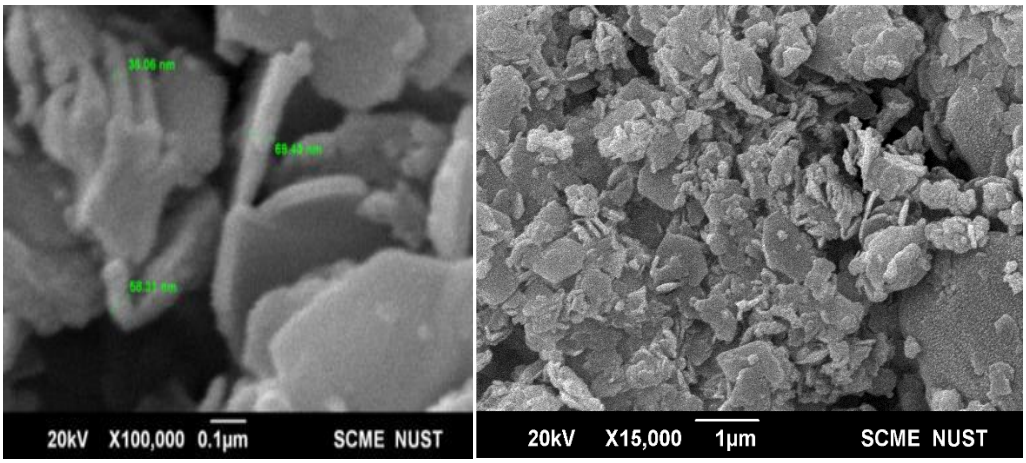

Figure 4 Electron micrograph of BZnO NPS

Wound healing potential of control groups

Statistically analyzed results showed that wound healing potential in male rat was more evident as compared to female rat in control groups as animals in the vehicle showed 77.08% wound healing, which may be because of the natural immunity of animals, while male animals in Group III showed 82.56% wound healing and female rats showed 91.45% (Figure 5 and Figure 6).

Wound Healing Potential of plant extracts and biogenic nanoparticles

Statistically analyzed results of showed after seven days, ether extract of *S. cumini* (Linn.) showed 55% wound healing, followed by its n-hexane extract which showed 50% wound healing in female rats. 37.5% wound healing was shown in male rats with water extract followed by the ethanolic extract (35% wound healing). After fourteen days, n-Hexane extract of *S. cumini* (Linn.) showed 92.5% wound healing in female rats followed by its ether and water extracts (90% wound closure in female and male rats respectively). 87.5% and 80% of wound closure has been observed in female and male rats respectively when they had been treated with water and n-hexane extracts respectively. After 21 days, all four extracts of *S.cumini*(Linn.) showed promising results with 100% wound closure in both male and female rats, followed by its ether and ethanolic extracts (90% and 85% wound closure respectively) in male rats. Among all extracts of *S.cumini*(Linn.) leaves, water extracts have significant wound closure in female rats as compared to male rats. Biogenic nanoparticles have shown wound contraction on each concentraion but after days 14 and 21 of nanoparticle application, wound contraction was almost same and results were similar to that of positive control drug (Figure 5 and Figure 6).

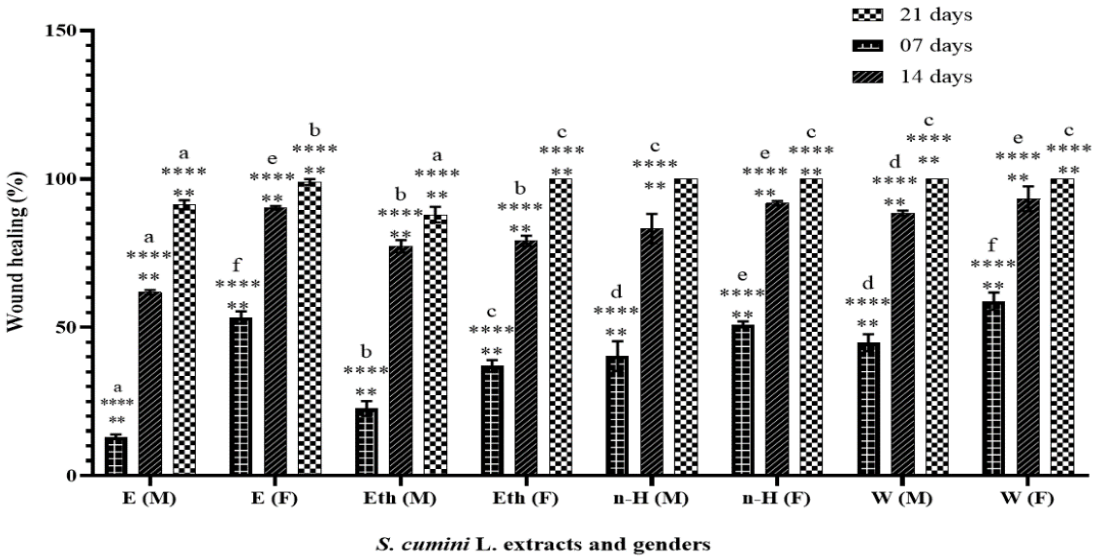

(A)

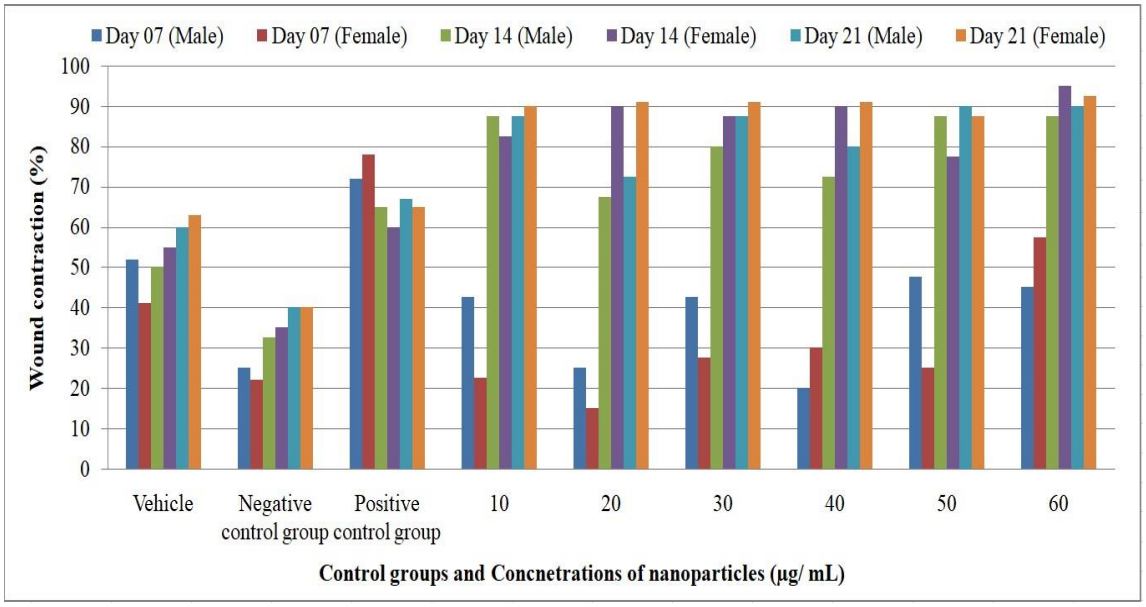

(B)

Figure 6: Wound healing effect on different genders of albino Wistar rats by (A) leaf extracts of *S.cumini* Linn. and (B) ZnO nanoparticles and Control groups

M= Male F= Female E= Ether extract, Eth= Ethanolic extract, n-H= n-Hexane extract, W= Water extract, **a** to **h** shows maximum to minimum wound healing efficacy (%)

** = Significant wound healing effect (%) on different days by leaf extracts of *S.cumini*(Linn.) at p= 0.0017, **** = Extremely significant wound healing effects (%) among different extracts of *S.cumini*Linn. at p< 0.0001.

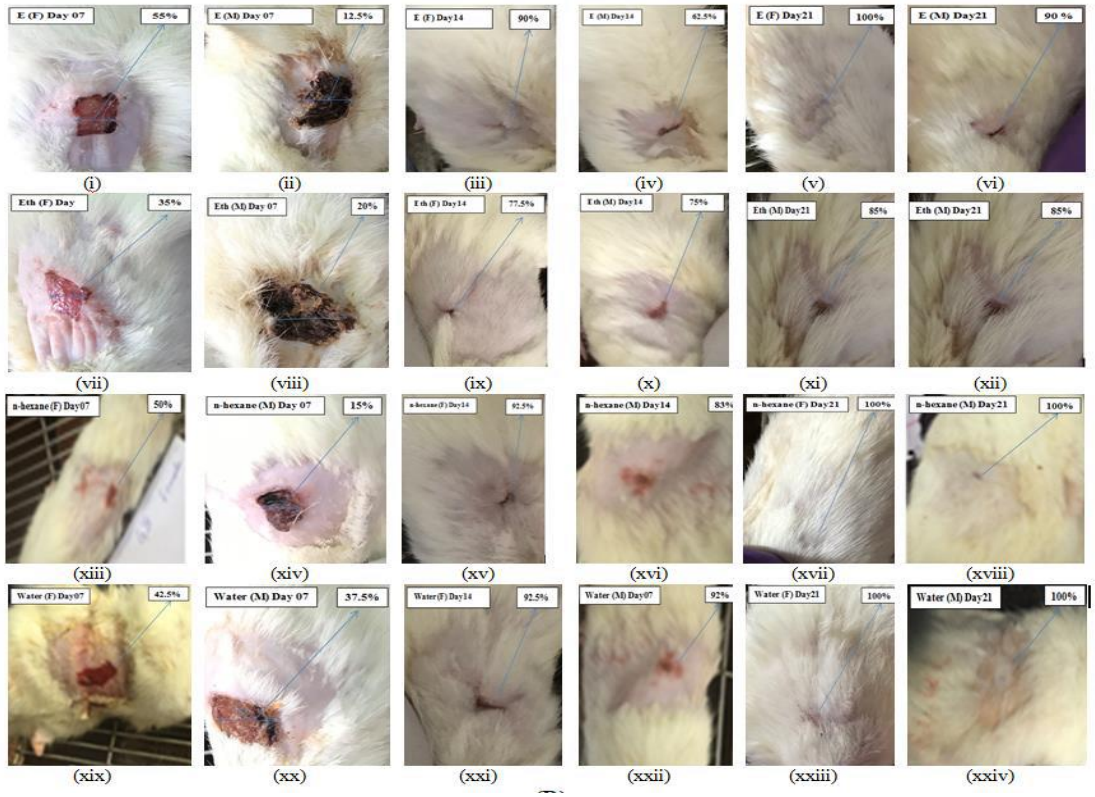
E (F) Day 07
55%
E (M) Day 07
12.5%
E (F) Day14
90%
E (M) Day14
62.5%
E (F) Day21
100%
E (M) Day21
90 %
(i)
(ii)
(iii)
(iv)
(v)
(vi)
Eth (F) Day
35%
Eth (M) Day 07
20%
Eth (F) Day14
77.5%
Eth (M) Day14
75%
Eth (M) Day21
85%
Eth (M) Day21
85%
(vii)
(viii)
(ix)
(x)
(xi)
(xii)
n-hexane (F) Day07
50%
n-hexane (M) Day 07
15%
n-hexane (F) Day14
92.5%
n-hexane (M) Day14
83%
n-hexane (F) Day21
100%
n-hexane (M) Day21
100%
(xiii)
(xiv)
(xv)
(xvi)
(xvii)
(xviii)
Water (F) Day07
42.5%
Water (M) Day 07
37.5%
Water (F) Day14
92.5%
Water (M) Day07
92%
Water (F) Day21
100%
Water (M) Day21
100%
(xix)
(xx)
(xxi)
(xxii)
(xxiii)
(xxiv)

(A)

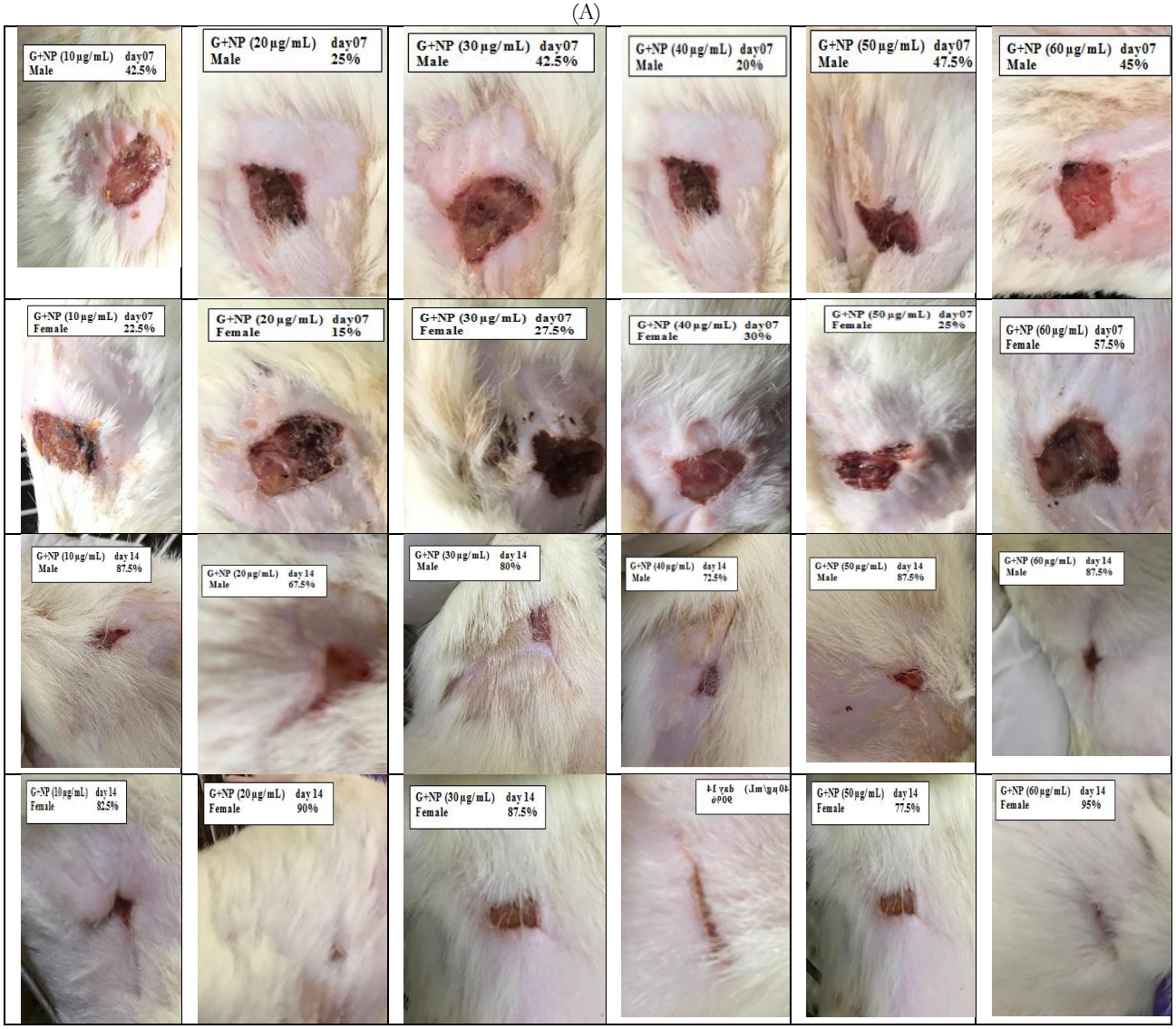
G+NP (10 µg/mL) day07
Male 42.5%
G+NP (20 µg/mL) day07
Male 25%
G+NP (30 µg/mL) day07
Male 42.5%
G+NP (40 µg/mL) day07
Male 20%
G+NP (50 µg/mL) day07
Male 47.5%
G+NP (60 µg/mL) day07
Male 45%
G+NP (10 µg/mL) day07
Female 22.5%
G+NP (20 µg/mL) day07
Female 15%
G+NP (30 µg/mL) day07
Female 27.5%
G+NP (40 µg/mL) day07
Female 30%
G+NP (50 µg/mL) day07
Female 25%
G+NP (60 µg/mL) day07
Female 57.5%
G+NP (10 µg/mL) day 14
Male 87.5%
G+NP (20 µg/mL) day 14
Male 67.5%
G+NP (30 µg/mL) day 14
Male 80%
G+NP (40 µg/mL) day 14
Male 72.5%
G+NP (50 µg/mL) day 14
Male 87.5%
G+NP (60 µg/mL) day 14
Male 87.5%
G+NP (10 µg/mL) day 14
Female 82.5%
G+NP (20 µg/mL) day 14
Female 90%
G+NP (30 µg/mL) day 14
Female 87.5%
G+NP (50 µg/mL) day 14
Female 77.5%
G+NP (60 µg/mL) day 14
Female 95%

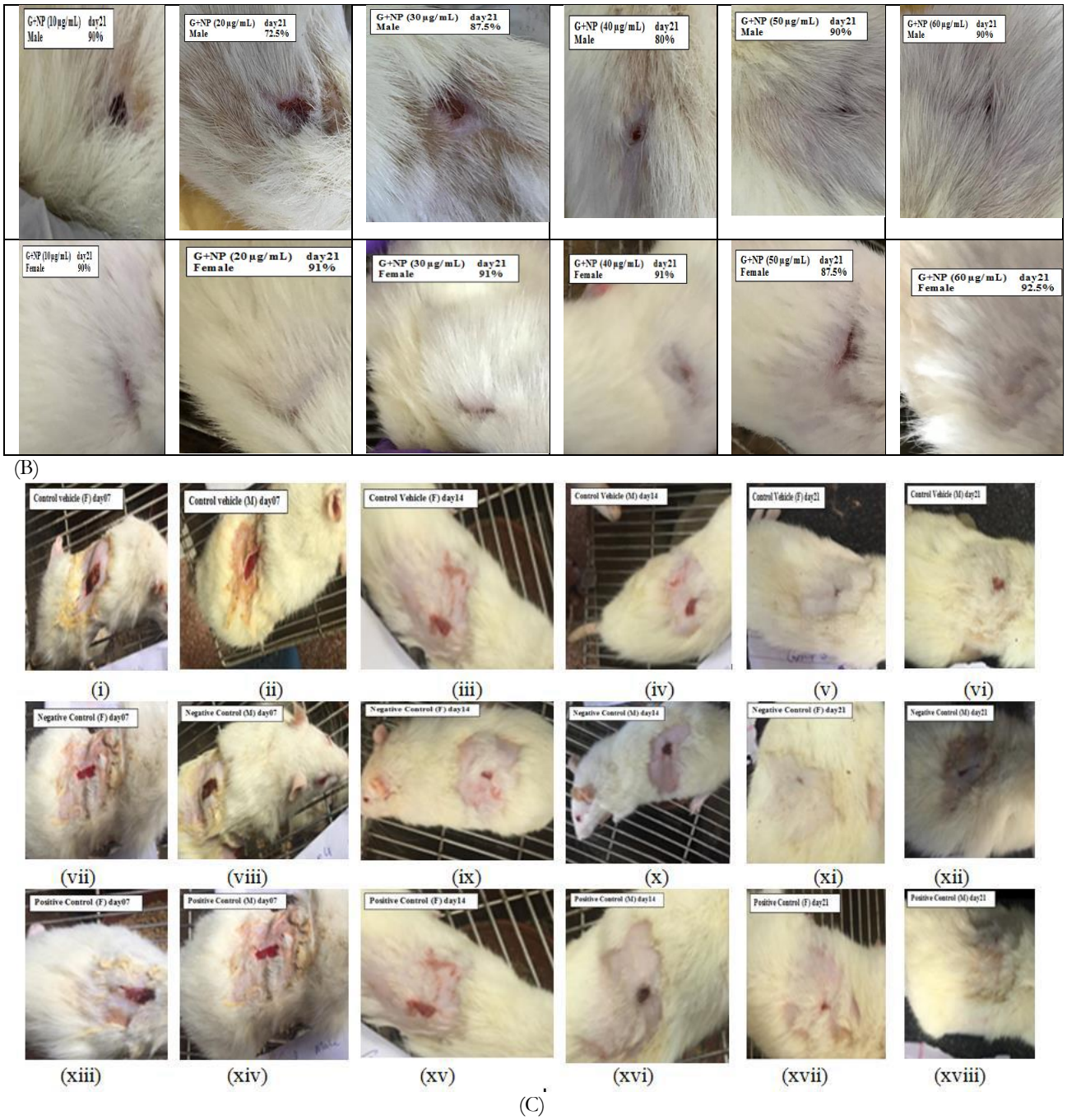

Figure 6: Wound healing effect (%)on different genders of albino Wistar rats (A) Leaf extracts of *S.cumini*(Linn.)**(B)**, ZnO nanoparticles **(C)** Control groups; M= Male F= Female E= Ether extract, Eth= Ethanolic extract, n-H= n-Hexane extract, W= Water extract, %**=** wound healing efficacy, G= Guaz, NP= Nanoparticles

DISCUSSION

Zinc oxide nanoparticles have been successfully synthesized using plant-based green extracts. A distinct change in color of the reaction mixture is a hallmark feature of zinc oxide nanoparticle formation, and numerous studies have reported this color change as the initial indication of nanoparticle synthesis. In agreement with previous research conducted by various experts, including, our study also observed a notable color change, confirming the successful synthesis of zinc oxide nanoparticles. This color change is a result of the reduction of zinc ions and the subsequent formation of zinc oxide nanoparticles, which exhibit unique optical properties due to their nanoscale size and high surface area Naseer et al., (2020) reported that Zinc oxide nanoparticles (ZnO NPs) were successfully synthesized using leaf extracts of Cassia fistula and Melia azedarach as reducing agents. The formation of ZnO NPs was confirmed by a distinct color change of the reaction mixture, which turned from yellow to light brown in the case of C. fistula extract and from red to off-white in the case of M. azedarach extract. This color change is a characteristic indication of the reduction of zinc ions and the subsequent formation of ZnO NPs, which exhibit unique optical properties due to their nanoscale size and high surface area

(Dihom et al., 2022). Zinc oxide nanoparticles (ZnO NPs) exhibited sharp and intense absorption peaks at wavelengths ranging from 360 to 363 nanometers, which is in excellent agreement with the findings of the present study. This

absorption profile is characteristic of ZnO NPs and confirms their successful synthesis. The peak positions and intensities observed in this study are consistent with previous reports, further validating the results (Salahuddin et al., 2015).
Results of present experimental study were in line with the previous study of Rajiv et al., (2013).
UV-Vis spectroscopy was employed as a secondary confirmation step to determine the nanoparticulate nature of the synthesized particles. The UV-Vis analysis revealed peak positions between 200-450 nm, which is a common range for nanoparticle absorption. Notably, the green-synthesized ZnO NPs exhibited a distinct peak position at 354 nm, attributed to the electron transition in the conduction band of the biofabricated ZnO NPs. This peak is characteristic of the large excitation binding energy of the nanoparticles at room temperature, further supporting their successful synthesis and nanoscale size. (Fakhari *et al.*, 2019). The size of nanoparticles plays a crucial role in changing the properties of materials, and UV-visible absorption spectroscopy is a widely used technique to study the optical properties of nanoparticles [1]. It is well known that the band gap increases as the particle size decreases, which is evident from absorption spectroscopy [1]. A study has also shown that ZnO nanoparticles prepared using Cassia fistula and Melia azedarach give peaks at 320 nm and 324 nm, respectively (Naseer et al., 2020). Similar results were also reported by study of Zhang et al (2002) and Swart et al., (2019). Results of band energy gap calculated by Tauc plot for the experimental nanoparticles were also in line with study of Xaba et al., 2019.
The XRD spectrum has prominent peaks corresponding to the diffraction peaks at 2θ = 31°, 34°, 36°, 47°, 56°, 62° and 67° were indexed with the diffraction planes (100), (002), (101), (102), (110), (103) and (112) approve with JCPDS card no. 36-1451, 63 which confirms the hexagonal wurtzite structure of ZnO NPs (Demissie et al., (2020). Results of present experimental analysis were in favor of Getie et al., (2017) and Gholamali and Yadollahi, (2021). Results of another study suggested that sharp peaks obtained by XRD analysis were used to calculate average size. Moroever NPs were hexagonal wurtzite in shape as reported by Dobrucka and Długaszewska (2016). SEM analysis was used for the morphological study of the experimental nanoparticles, as reported by experts (Rajiv et al., 2013).
Wound healing is dynamic process and complicated that restores cellular structures and tissue layers in damaged tissue to their normal state at its best. Wound contracture is a condition that happens throughout the healing process, beginning with the fibroblastic stage, in which the wound shrinks. Hemostasis and inflammation characterize the inflammatory phase, which is followed by epithelialization, angiogenesis, and collagen deposition in the proliferative phase. The wound contracts during the maturational phase, the final stage of wound healing, results in lower quantity of apparent scar tissue (Nilesh *et al.,* 2010).
Somwanshi, S.B., and Hiremath, S. N. (2018) found that the use of herbal plants, which are generally less toxic, allows for prolonged administration. Polyherbal medications, which contain multiple plant constituents (Table 2 and Figure 7), offer advantages over synthetic chemicals due to their synergistic effects on wound healing. These phytochemicals possess anti-inflammatory, antioxidant, and antimicrobial properties, leading to enhanced efficacy and reduced adverse reactions. Therefore, rigorous scientific investigation is crucial to explore the pharmacological applications of herbal medicines and validate the claims made about them in traditional remedies.
The proliferative phase of wound healing is characterized by collagen accumulation, granulation, epithelialization, and wound contraction. Myofibroblasts play a crucial role in wound contraction, while epithelial cells migrate across the wound site to facilitate healing. Wound contraction occurs throughout the healing process, and studies have shown that extracts of A. indica, A., and N. tabacum L. accelerate wound contraction and epithelialization, leading to improved collagen synthesis and effective healing (Shivanand*aet al.,* 2014).
Collagen, a crucial component of connective tissues, plays a vital role in wound healing by providing a scaffold for regenerative tissues. Composed primarily of the amino acid hydroxyproline, collagen is a key component of the extracellular matrix, imparting strength and support to tissues. The methanolic extract significantly enhanced wound contraction in the experimental group compared to the control group, suggesting that it may accelerate collagen synthesis, leading to faster wound healing., which is attributed to the phytocompounds in Methanolic extracts of plant (Table 2) (Samanta*et al.,* 2016). The phyto-extracts of Syzygiumcumini Linn. leaves, obtained using various solvents such as ether, ethanol, n-hexane, and water, have demonstrated significant wound healing activity. This is attributed to the presence of phytochemicals, including tannins, flavonoids, and phenolic compounds, which have been reported to possess anti-inflammatory, antioxidant, antimicrobial, and immunomodulatory properties. These bioactive compounds can promote wound healing by (Table 2). These phytochemicals are effective in promoting wound healing by increasing the rate of healing, reducing inflammation, and providing protection against infection (Kumar &Ahirwar 2017).

Table 2 Phyto-compounds and their properties in polarity based extracts of *S. cumini* Linn. leaf extract

Compounds	Molecular formulas	Molecular weights (g/mole)	Structures (Figure 7)	Solubility in water	Pubchem ID
Saponins	$C_{58}H_{94}O_{27}$	1223.3	a	Polar/ Soluble	198016
Quinones	$C_{15}H_{14}O_6$	290.27	B	Less polar/ less soluble	11437738
Oxalic acid	$C_2H_2O_4$	90.03	C	Polar/ Soluble	12252960
Gallic acid	$C_7H_6O_5$	170.12	d	Polar/ Soluble	288114
Taxifolin	$C_{15}H_{12}O_7$	304.25	E	Polar/ Soluble	439533
Methyl gallate	$C_8H_8O_5$	184.17	F	Polar/ Soluble	7428
Quercetin	$C_{15}H_{10}O_7$	302.236	g	Polar/ Soluble	5280343
Luteolin	$C_{15}H_{10}O_6$	286.24	H	Polar/ Soluble	5280445
Hesperidin	$C_{28}H_{34}O_{15}$	610.565	I	Less polar/ less soluble	10621

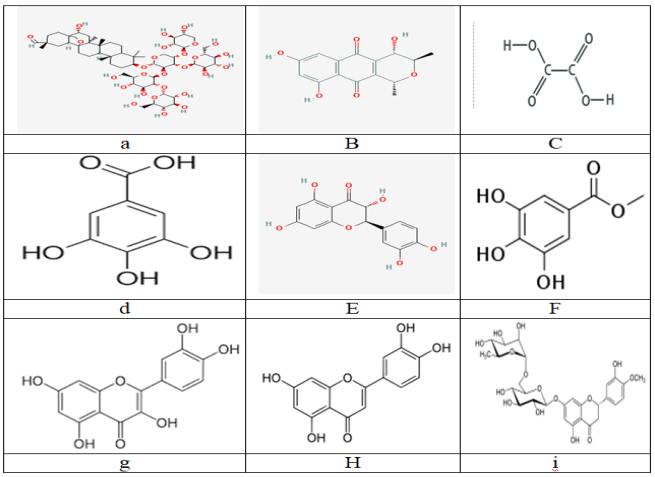

Figure 7 Major phytocompounds in different extracts of *S.cumini* (Linn.) leaves (Qamar *et al.,* 2022, Singh et al., 2019, Samanta et al. , 2016, Sudheesh et al. , 2012 and Banumathi et al. , 2017)

CONCLUSION

The leaf extracts of Jambolana (*Syzygium cumini* Linn.) were successfully used to synthesize zinc oxide nanoparticles (ZnO NPs), which were stabilized and capped by the plant extracts. The prepared nanoparticles were characterized using UV, FTIR, XRD, and SEM analysis, confirming their nanostructure and stability. The FTIR analysis revealed that the plant extracts played a crucial role in the successful synthesis and stability of the nanoparticles. The nanoparticles had an average size of around 70 nm with an irregular shape. The wound healing activity of the S. cumini leaf extracts and BZnO nanoparticles was evaluated in female and male rats. The results showed that all extracts except n-hexane extract exhibited significant wound healing activity, with the ethanolic and water extracts showing maximum activity. The BZnO nanoparticles of leaf extract showed maximum wound healing activity at a concentration of 40 µg/mL, with the maximum activity observed after two weeks of application. The wound contraction activity is attributed to the polar compounds present in the ethanolic and water extracts of the plant. The study highlights the potential of *S. cumini* leaf extracts and BZnO nanoparticles for wound healing applications, and their value for advanced studies in various branches of science.

Competing Interests

N/A

Acknowledgement

All authors are highly acknowledged to Government of Pakistan which have approved the the host institution and Higher Education Commission (HEC) Pakistan, under the umbrella of which HEC approved Ph.D. faculty has executed this project as a part of Ph.D. thesis.

Funding Source

N/A

Author contribution

HW= Performed all experimental work of project as a part of her Ph.D. thesis work, BR: Provided her financial support to bear the expenses of current work. AA= Supervised the whole project, Proofread the manuscript, and provided final approval of manuscript. RB= Prepared the 1st and last draft of manuscript and provided her English editing services to write the manuscript. SH= Provided her technical support in drafting the manuscript and provided her English editing services. BI= Provided his technical support in writing the 2nd last draft manuscript. NI= Co-supervised during nanoparticle synthesis and characterization and provided his technical support in the interpretation of the results.

References

1. Abubakar AR, Haque M. (2020). Preparation of medicinal plants: Basic extraction and fractionation procedures for experimental purposes. Journal of Pharmacy &Bioallied Sciences; 12 (1): 1.
2. Banozic, M, Banjari I, Jakovljević M, Subaric D, Tomas S, Babic, J, &Jokic, S. (2019). Optimization of ultrasound-assisted extraction of some bioactive compounds from *N. tabacum* (L.) waste. *Molecules*; *24*(8): 1611.
3. Banozic, M, Subaric, D, Jokic S, (2018). *N. tabacum* (L.) waste in Bosnia and Herzegovina–problem or high-value material? Glasnikzastitebilja 4; 24–33.
4. Cvetanovska A, Krstic M, Cvetanovska L, (2017). Content of total phenolic compounds and antioxidant potential of oriental *N. tabacum* (L.) varieties (*Nicotiana tabacum* (L.). European Journal of Pharmaceutical and Medical Research; 4, 2223–2228.
5. Dogan KH (Ed.) (2019). Wound Healing: Current Perspectives.

6. El-Sakhawy MA, Soliman GA, El-Sheikh HH, &Ganaie MA (2023). Anticandidal effect of *Eucalyptus globulus* oil and three isolated compounds on cutaneous wound healing in rats. European Review for Medical and Pharmacological Sciences; *27*, 26-37.
7. Fabio G, Romanucci V, Marino C, Pisanti A, and Zarrelli A &Gymnemasylvestre R Br, (2015). An Indian medicinal herb: traditional uses, chemical composition, and biological activity. Current Pharmaceutical Biotechnology; 16(6) 506–516 2015.
8. Jayalakshmi MS, Thenmozhi P, &Vijayaraghavan R. (2021). Plant leaves extract irrigation on wound healing in diabetic foot ulcers. *Evidence-Based Complementary and Alternative Medicine*; 1-9.
9. Mohandas A, Sudheesh Kumar PT, Raja B, Lakshmanan, VK, & Jayakumar R. (2015). Exploration of alginate hydrogel/nano zinc oxide composite bandages for infected wounds. International journal of nanomedicine; 10(Suppl 1), 53.
10. Nilesh S, Amit J, Vaishali U, Sujit K, Sachin K, & Ravindra P. (2010). Protective effect of *Lepidium sativum* against doxorubicin-induced nephrotoxicity in rats. *Research Journal of Pharmaceutical Biological and Chemical Sciences*; *1*(3), 42-49.
11. Qamar M, Akhtar S, Ismail T, Wahid M, Abbas MW, Mubarak MS, &Esatbeyoglu T (2022). Phytochemical Profile, Biological Properties, and Food Applications of the Medicinal Plant *Syzygiumcumini*. *Foods*; *11*(3), 378.
12. Ravindran J, Arumugasamy V, & Baskaran A. (2019). Wound healing effect of silver nanoparticles from *Tridax procumbens* leaf extracts on Pangasius hypophthalmus. *Wound Medicine*; *27*(1), 100170.
13. Samanta R, Pattnaik AK, Pradhan KK, Mehta BK, Pattanayak SP, and Banerjee S. (2016). Wound healing activity of silibinin in mice. *Pharmacognosy research*; *8*(4), 298.
14. Sharma A, Khanna S, Kaur G, & Singh I. (2021). Medicinal plants and their components for wound healing applications. *Future Journal of Pharmaceutical Sciences*; *7*(1), 1-13.
15. Somwanshi SB, and Hiremath, SN. (2018). *In-vivo* Evaluation of the Wound Healing Activity of the *Sesamum Indicum* L. Seed Extract in Novel Ethosomal Vesicular System. *Journal of Drug Delivery and Therapeutics*; *8*(5), 411-420.
16. Sourirajan A, Dev K, & Kumar V. (2020). Comparison of extraction yield, phytochemicals and *in vitro* antioxidant potential of different extracts of two Ficus species. *Plant Archives*; *20*(1), 2669-2673.
17. Sudheesh Kumar PT, Lakshmanan VK, Anilkumar TV, Ramya C, Reshmi P, Unnikrishnan AG, & Jayakumar R. (2012). Flexible and microporous chitosan hydrogel/nano ZnO composite bandages for wound dressing: *in vitro* and *in vivo* evaluation. *ACS applied materials & interfaces*; *4*(5), 2618-2629.
18. Badar, R., Ahmed, A., Munazir, M. et al. Wheat leaf rust control through biofabricated zinc oxide nanoparticles. Australasian Plant Pathol. (2023). https://doi.org/10.1007/s13313-023-00949-1
19. Banumathi, B., Vaseeharan, B., Ishwarya, R., Govindarajan, M., Alharbi, N. S., Kadaikunnan, S., ...&Benelli, G. (2017). Toxicity of herbal extracts used in ethno-veterinary medicine and green-encapsulated ZnO nanoparticles against *Aedes aegypti* and microbial pathogens. Parasitology research, 116(6), 1637-1651.
20. Benelli, G., Maggi, F., Pavela, R., Murugan, K., Govindarajan, M., Vaseeharan, B. & Higuchi, A. (2018). Mosquito control with green nanopesticides: towards the One Health approach? A review of non-target effects. Environmental Science and Pollution Research, 25(11), 10184-10206.
21. Bratovcic, A. (2019). Different applications of nanomaterials and their impact on the environment. SSRG International Journal of Material Science and Engineering, 5(1), 1-7.
22. Chaudhary, A., Kumar, N., Kumar, R., &Salar, R. K. (2019). Antimicrobial activity of zinc oxide nanoparticles synthesized from Aloe vera peel extract. SN Applied Sciences, 1(1), 1-9.
23. Dihom, H. R., Al-Shaibani, M. M., Mohamed, R. M. S. R., Al-Gheethi, A. A., Sharma, A., &Khamidun, M. H. B. (2022). Photocatalytic degradation of disperse azo dyes in textile wastewater using green zinc oxide nanoparticles synthesized in plant extract: A critical review. Journal of Water Process Engineering, 47, 102705.
24. Divya, M., Vaseeharan, B., Abinaya, M., Vijayakumar, S., Govindarajan, M., Alharbi, N. S.,&Benelli, G. (2018). Biopolymer gelatin-coated zinc oxide nanoparticles showed high antibacterial, antibiofilm and anti-angiogenic activity. Journal of Photochemistry and Photobiology B: Biology, 178, 211-218.
25. Dobrucka, R., &Długaszewska, J. (2016). Biosynthesis and antibacterial activity of ZnO nanoparticles using Trifolium pratense flower extract. Saudi journal of biological sciences, 23(4), 517-523.
26. Gade, A., Ingle, A., Whiteley, C., & Rai, M. (2010). Mycogenic metal nanoparticles: progress and applications. Biotechnology letters, 32, 593-600.
27. Gajanan, K., & Tijare, S. N. (2018). Applications of nanomaterials. Materials Today: Proceedings, 5(1), 1093-1096.
28. Getie, S., Belay, A., Chandra Reddy, A. R., & Belay, Z. (2017). Synthesis and characterizations of zinc oxide nanoparticles for antibacterial applications. J NanomedNanotechno S, 8(004).
29. Gholamali, I., &Yadollahi, M. (2021). Bio-nanocomposite polymer hydrogels containing nanoparticles for drug delivery: A review. Regenerative Engineering and Translational Medicine, 7, 129-146.
30. Ishwarya, R., Vaseeharan, B., Kalyani, S., Banumathi, B., Govindarajan, M., Alharbi, N. S., &Benelli, G. (2018). Facile green synthesis of zinc oxide nanoparticles using Ulva lactuca seaweed extract and evaluation of their photocatalytic, antibiofilm and insecticidal activity. Journal of Photochemistry and Photobiology B: Biology, 178, 249-258.
31. Jamdagni, P., Khatri, P., & Rana, J. S. (2018). Green synthesis of zinc oxide nanoparticles using flower extract of Nyctanthes arbor-tristis and their antifungal activity. Journal of King Saud University-Science, 30(2), 168-175.
32. Karthika, V., Arumugam, A., Gopinath, K., Kaleeswarran, P., Govindarajan, M., Alharbi, N. S., ...&Benelli, G. (2017). Guazumaulmifolia bark-synthesized Ag, Au and Ag/Au alloy nanoparticles: Photocatalytic potential, DNA/protein interactions, anticancer activity and toxicity against 14 species of microbial pathogens. Journal of Photochemistry and Photobiology B: Biology, 167, 189-199.

33. Khot, L. R., Sankaran, S., Maja, J. M., Ehsani, R., & Schuster, E. W. (2012). Applications of nanomaterials in agricultural production and crop protection: a review. Crop protection, 35, 64-70.
34. Naseer, M., Aslam, U., Khalid, B., & Chen, B. (2020). Green route to synthesize Zinc Oxide Nanoparticles using leaf extracts of Cassia fistula and Melia azadarach and their antibacterial potential. Scientific Reports, 10(1), 9055.
35. Rajapriya, M., Sharmili, S. A., Baskar, R., Balaji, R., Alharbi, N. S., Kadaikunnan, S., ...&Vaseeharan, B. (2019). Synthesis and characterization of zinc oxide nanoparticles using Cynarascolymus leaves: Enhanced hemolytic, antimicrobial, antiproliferative, and photocatalytic activity. Journal of Cluster Science, 31(4), 791-801.
36. Rajiv, P., Rajeshwari, S., &Venckatesh, R. (2013). Bio-Fabrication of zinc oxide nanoparticles using leaf extract of Parthenium hysterophorus L. and its size-dependent antifungal activity against plant fungal pathogens. Spectrochimica Acta Part A: Molecular and Biomolecular Spectroscopy, 112, 384-387.
37. Rajiv, P., Rajeshwari, S., &Venckatesh, R. (2013). Bio-Fabrication of zinc oxide nanoparticles using leaf extract of Parthenium hysterophorus L. and its size-dependent antifungal activity against plant fungal pathogens. Spectrochimica Acta Part A: Molecular and Biomolecular Spectroscopy, 112, 384-387.
38. Roduner, E. (2006). Size matters: why nanomaterials are different. Chemical society reviews, 35(7), 583-592.
39. Salahuddin, N. A., El-Kemary, M., & Ibrahim, E. M. (2015). Synthesis and characterization of ZnO nanoparticles via precipitation method: effect of annealing temperature on particle size. Nanosci. Nanotechnol, 5(4), 82-88.
40. Santhoshkumar, J., Kumar, S. V., &Rajeshkumar, S. (2017). Synthesis of zinc oxide nanoparticles using plant leaf extract against urinary tract infection pathogen. Resource-Efficient Technologies, 3(4), 459-465. 24. Sharma, J., Sweta, Thakur, C., Vats, M., & Sharma, S. K. (2020, May). Green synthesis of zinc oxide nanoparticles using neem extract. In AIP Conference Proceedings (Vol. 2220, No. 1, p. 020107). AIP Publishing LLC.
41. Singh, T., Jyoti, K., Patnaik, A., Singh, A., Chauhan, R., &Chandel, S. S. (2017). Biosynthesis, characterization and antibacterial activity of silver nanoparticles using an endophytic fungal supernatant of Raphanussativus. Journal of Genetic Engineering and Biotechnology, 15(1), 31-39.
42. Singh, Y., Bhatnagar, P., & Kumar, S. (2019). A review on bio-active compounds and medicinal strength of Jamun (SyzygiumcuminiSkeels. IJCS, 7(4), 3112-3117.
43. Swart, H. C., & Kroon, R. E. (2019). Ultraviolet and visible luminescence from bismuth doped materials. Optical Materials: X, 2, 100025.
44. Vijayakumar, S., Vaseeharan, B., Malaikozhundan, B., &Shobiya, M. (2016). Laurusnobilis leaf extract mediated green synthesis of ZnO nanoparticles: characterization and biomedical applications. Biomedicine & Pharmacotherapy, 84, 1213-1222.
45. Xaba, T., Mongwai, P. P., &Lesaoana, M. (2019). Decomposition of bis (N-benzyl-salicydenaminato) zinc (II) complex for the synthesis of ZnO nanoparticles to fabricate ZnO-chitosan nanocomposite for the removal of iron (II) ions from wastewater. Journal of Chemistry, 1-9.
46. Zhang, D. H., Xue, Z. Y., & Wang, Q. P. (2002). The mechanisms of blue emission from ZnO films deposited on glass substrate by rf magnetron sputtering. Journal of Physics D: Applied Physics, 35(21), 2837.